CFD modeling of condensation process of water vapor in supersonic flows

Yan Yang [a], Jens Honore Walther [b,c], Yuying Yan [d], Chuang Wen [a,b,*]

[a] School of Petroleum Engineering, Changzhou University, Changzhou 213016, China
[b] Section of Fluid Mechanics, Coastal and Maritime Engineering, Department of Mechanical Engineering, Technical University of Denmark, Nils Koppels Allé, 2800 Kgs. Lyngby, Denmark
[c] Chair of Computational Science, ETH Zürich, Clausiusstrasse 33 ETH-Zentrum, CLT F 11, CH-8092 Zürich, Switzerland
[d] Faculty of Engineering, University of Nottingham, University Park, Nottingham NG7 2RD, UK

HIGHLIGHTS

- CFD modeling is developed to predict spontaneous condensation in supersonic flows.
- Spontaneous condensation does not appear immediately with saturation state of steam.
- Condensation process occurs further downstream the throat of supersonic nozzle.

ARTICLE INFO

ABSTRACT

The condensation phenomenon of vapor plays an important role in various industries, such as the steam flow in turbines and refrigeration system. A mathematical model is developed to predict the spontaneous condensing phenomenon in the supersonic flows using the nucleation and droplet growth theories. The numerical approach is validated with the experimental data, which shows a good agreement between them. The condensation characteristics of water vapor in the Laval nozzle are described in detail. The results show that the condensation process is a rapid variation of the vapor-liquid phase change both in the space and in time. The spontaneous condensation of water vapor will not appear immediately when the steam reaches the saturation state. Instead, it occurs further downstream the nozzle throat, where the steam is in the state of supersaturation.

1. Introduction

The condensation phenomenon of vapor plays an important role in various industries, such as the steam flow and water vapor in nozzles [1], turbines [2], ejectors [3], thermos-compressors [4] and supersonic separators [5–9]. Theoretical and experimental studies have been conducted for the condensation process in supersonic flows, focusing on the nucleation theory, droplet size, latent heat [10–12]. Numerical simulations have been performed to predict the condensing flow with the development of the computational fluid dynamics (CFD) for several decades.

Hill [13], Noori Rahim Abadi et al. [14] studied the nucleation process of wet steam flows in nozzles at low and high pressure,

respectively. White and Young predicted the condensing process using Eulerian-Lagrangian and time-marching methods [15]. Gerber [16] developed the Eulerian-Lagrangian and Eulerian-Eulerian two-phase models for predicting the condensation flow with the classical nucleation theory. The effects of friction factor on the condensation flows in the Laval nozzles were performed using the single fluid model by Mahpeykar and Teymourtash [17], and Jiang et al. [18]. Two-dimensional simulation of the condensing steam was calculated in converging-diverging nozzles using a Jameson-style finite volume method on an unstructured and adaptive triangular mesh [19]. Yang and Sheng [20] described a conservative two-dimensional compressible numerical model for the non-equilibrium condensing of the steam flow based on the classical nucleation theory and the Virial type equation of state. The effect of the expansion rate on the steam condensing flow through a converging-diverging nozzle was studied numerically by Nikkhahi et al. [21]. The steam condensing flow was modeled through the Laval nozzles at low and high inlet pressures by means of the

* Corresponding author at: Section of Fluid Mechanics, Coastal and Maritime Engineering, Department of Mechanical Engineering, Technical University of Denmark, Nils Koppels Allé, 2800 Kgs. Lyngby, Denmark.
E-mail address: cwen@mek.dtu.dk (C. Wen).

single-fluid model [22]. The Eulerian-Eulerian approach was adopted for modeling the condensing steam flow, and the simulation was conducted on the commercial ANSYS FLUENT 12.1 platform [23].

The condensation phenomenon of water vapor in supersonic flows is still not understood very well as a result of the complex phase change process. Especially, the numerical simulation depends on various nucleation theories and droplet growth models. In this paper, the Euler-Euler two-phase flow model is developed to predict the spontaneous condensing phenomenon in the Laval nozzle. The modified internally consistent classic nucleation theory and Gyarmathy's droplet growth model are employed to perform the simulation cases. The numerical approach is validated with experimental data. The condensation process of water vapor is numerically analyzed in detail, including the nucleation rate, droplet numbers, droplet radius and droplet fraction.

2. Mathematical model

2.1. Governing equations

For the water vapor condensation in a Laval nozzle, the fluid flow is governed by partial differential equations describing the conservation of mass, momentum and energy, as shown in Eqs. (1–3).

$$\frac{\partial \rho}{\partial t} + \frac{\partial(\rho u_j)}{\partial x_j} = S_m \tag{1}$$

$$\frac{\partial}{\partial t}(\rho u_i) + \frac{\partial}{\partial x_j}(\rho u_j u_i) = -\frac{\partial p}{\partial x_i} + \frac{\partial \tau_{ij}}{\partial x_j} + S_{u_i} \tag{2}$$

$$\frac{\partial}{\partial t}(\rho H) + \frac{\partial}{\partial x_j}(\rho u_j H + p) = -\frac{\partial}{\partial x_j}\left(\lambda_{eff}\frac{\partial T}{\partial x_j}\right) + \frac{\partial}{\partial x_j}(u_i \tau_{ij}) + S_{h_i} \tag{3}$$

where ρ, u, p and H are the density, velocity, pressure and total enthalpy, respectively. λ_{eff} and T are the effective heat conductivity and temperature. The source terms, S_m, S_{u_i}, S_{h_i}, are needed in these equations to consider the effect of the condensation process.

Additionally, two transport equations are employed to describe the phase change process during the condensation of the water vapor. In this simulation, the conservation equations include the liquid fraction (Y) and droplet number (N), which can be given by:

$$\frac{\partial(\rho Y)}{\partial t} + \frac{\partial}{\partial x_j}(\rho Y u_j) = S_Y \tag{4}$$

$$\frac{\partial(\rho N)}{\partial t} + \frac{\partial}{\partial x_j}(\rho N u_j) = \rho J \tag{5}$$

where the source term S_Y describes the condensation rate of the water vapor, and J is the nucleation rate, respectively.

The source term can be defined as follows:

$$S_m = -S_Y = -\dot{m} \tag{6}$$

$$S_{u_i} = -\dot{m}u_i \tag{7}$$

$$S_{h_i} = -\dot{m}h_i \tag{8}$$

$$\dot{m} = \frac{4\pi r^{*3}}{3}\rho_l J + 4\pi r^2 \rho_l N \frac{dr}{dt} \tag{9}$$

where $\dot{m}$ is the condensation mass per unit vapor volume per unit time. ρ_l is the droplet density, r is the droplet radius. dr/dt is the growth rate of droplets. The r^* is the Kelvin-Helmholtz critical droplet radius, which can be given by

$$r^* = \frac{2\sigma}{\rho_l R_v T \ln(S)} \tag{10}$$

where S is the super saturation ratio, defined as the ratio of vapor pressure to the equilibrium saturation pressure.

The nucleation rate, J, can be calculated by the internally consistent classic nucleation theory (ICCT) [24], which predicts the nucleation process of the water vapor as follows:

$$J = \frac{\zeta}{S}\frac{\rho_v^2}{\rho_l}\sqrt{\frac{2\sigma}{\pi m_v^3}}\exp\left(-\frac{16\pi}{3}\frac{\sigma^3}{k_B^3 T_v^3 \rho_l^2 (\ln S)^2}\right)\exp(\Theta) \tag{11}$$

where σ is the liquid surface tension, m_v is the mass of a vapor molecule, k_B is the Boltzmann's constant, T_v is the vapor temperature, ζ is a correction factor, Θ is a dimensionless surface tension.

$$\Theta = \frac{\sigma a_0}{k_B T_v} \tag{12}$$

where a_0 is the molecular surface area.

The growth rate of droplets due to evaporation and condensation, dr/dt, is calculated by Gyarmathy's model by [25],

$$\frac{dr}{dt} = \frac{\lambda_v(T_s - T_v)}{\rho_l h}\frac{(1 - r^*/r)}{\left(r + \frac{\sqrt{8\pi}}{1.5Pr}\frac{\gamma}{\gamma+1}l\right)} \tag{13}$$

where λ_v is the heat conductivity coefficient of the vapor, h is the vapor specific enthalpy, T_s is the saturated steam temperature, γ is the vapor adiabatic exponent, Pr is the Prandtl number.

2.2. Turbulence model

Depending on the information required, different turbulence models can be applied for the numerical simulation of supersonic flows, from k-ε model [26–28], Shear Stress Turbulent (SST) k-ω [29], Large Eddy Simulation (LES) to Direct Numerical Simulation (DNS). In this paper, the k-ε turbulence model is used to predict the supersonic flows. The equations for the turbulence model are not documented here for brevity, but are however well documented elsewhere [30].

2.3. Numerical schemes

The commercial package ANSYS FLUENT 17 is employed as the computational platform. The conservation equations (1)–(3) for vapor phase are directly solved in FLUENT, while the governing equations (4)–(13) for liquid phase and the source terms are performed with C code by the User-Defined-Scalar (UDS) and User-Defined-Function (UDF) interfaces. The SIMPLE algorithm [31] is used to couple the velocity field and pressure. The second-order upwind scheme is adopted for an accurate prediction. The transient state solution is used in the numerical studies with a time step of 10^{-6} s. The inlet conditions for the nozzle entrance are chosen from experimental tests including total pressure and total temperature. Since the flow is supersonic at the nozzle outlet, the pressure at the outlet does not influence the solution and is assigned an arbitrary low value. The convergence criterion for the relative residual of the continuity and all other dependent variables is set to 10^{-3} and 10^{-6}, respectively. The mass imbalance value is assigned as 10^{-4} to ensure iteration convergence.

3. Results and discussion

The validation, verification and implementation of the numerical studies are conducted using the geometry and experimental data from the available literature by Moses and Stein [12]. In their studies, the Laval nozzle was employed to experimentally study the condensation process of water vapor in supersonic flows. The

nozzle throat is located at $x = 82.2$ mm with the dimension of 10.0 mm (height) $\times$ 10.0 mm (depth). A sketch of the geometry of the Laval nozzle used in the experiments is described in Fig. 1. The subsonic part is composed of an arc with a radius of 53.0 mm, while the transonic and supersonic parts consist of an arc with a radius of 686.0 mm.

3.1. Grid independence tests

The grid density is one of the key factors that determines the accuracy of the numerical simulation. Three different densities of the structural grids are used to test the grid independence, including the coarse (8640 cells), medium (23,040 cells), fine (51,840 cells) and very fine (246,400) grids. The static pressure and temperature at the nozzle inlet for the simulations are 54702.17 Pa and 373.15 K, respectively. One of the condensation parameters, the nucleation rate, is selected to evaluate the effect of the grid density on the condensation simulation. The nucleation rate along the axis of the Laval nozzle is shown in Fig. 2. We can see that the nucleation rate calculated from the coarse grid significantly deviates from other cases, while the medium, fine and very fine grids represent similar results. Therefore, the grid system with 23,040 cells is used to conduct our simulations considering the computing accuracy and efficiency.

3.2. Model validation

The static pressure is firstly compared between the numerical and experimental data at the inlet pressure of 54702.17 Pa and inlet temperature of 373.15 K. The numerical result of the static pressure is shown in Fig. 3, and the value at the central line is employed for the data validation. Fig. 4 depicts the dimensionless pressure, defined as the ratio of local static pressure to the inlet one, along the central axis of the Laval nozzle. We can see that the predicted onset of the condensation process at $x = 104$ mm, occurs earlier than the experimental test at $x = 107$ mm. The increase of the static pressure due to the condensing flow in the simulation is smaller than the experiments.

Then, the droplet fraction due to the condensation process is employed to validate the numerical model. The pressure and temperature at the nozzle inlet are 40050.04 Pa and 374.30 K, respectively. Fig. 5 shows the numerical and experimental data of the droplet fraction along the axis in the Laval nozzle. The numerical model predicts the droplet fraction in supersonic flows, although
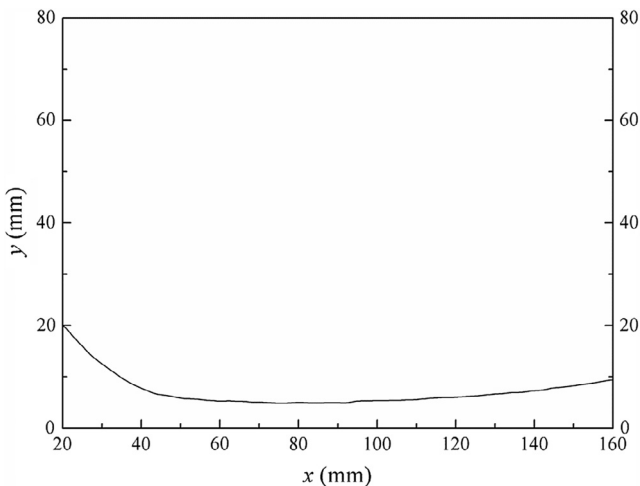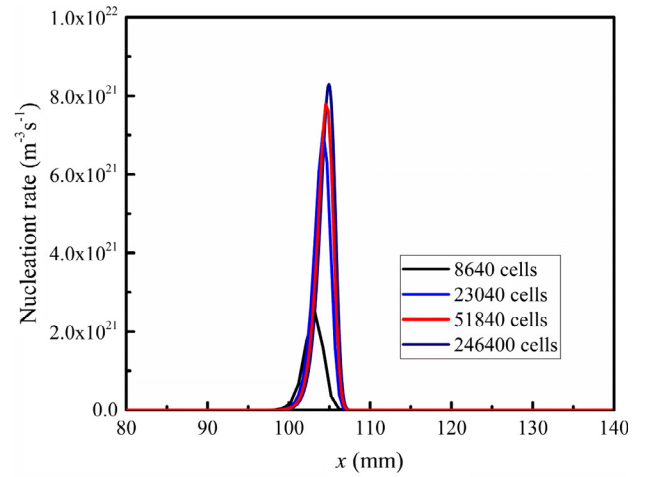

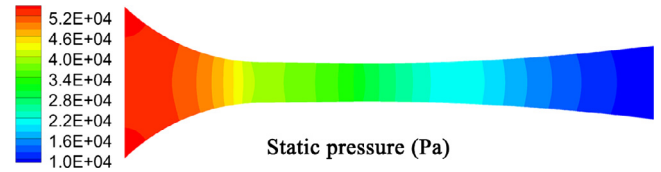**Fig. 2.** Effect of grid density on nucleation rate in supersonic flows.

Fig. 3. Numerical results of static pressure in the Laval nozzle.
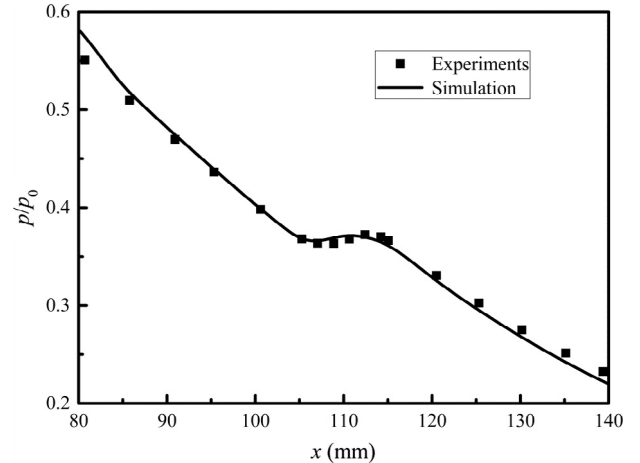

Fig. 4. Numerical and experimental results of static pressure at the central line of the Laval nozzle.

almost all of the numerical results are less than the experimental data.

Generally, the numerical model is validated in detail by comparing the static pressure and droplet fraction during the condensation process in the Laval nozzle. The comparison results demonstrate that the numerical model can accurately capture the condensation process of the water vapor in the Laval nozzle.

3.3. Condensation process

In this section, the condensation process of the water vapor is numerically calculated in the above mentioned Laval nozzle at the inlet pressure of 54702.17 Pa and temperature of 373.15 K, respectively. Fig. 6 shows the computational contours of the Mach number in the Laval nozzle, and the detailed information at the
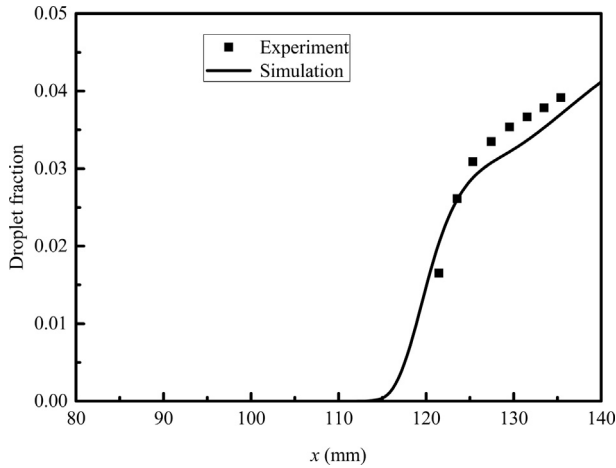

Fig. 1. Geometry and size of the Laval nozzle.

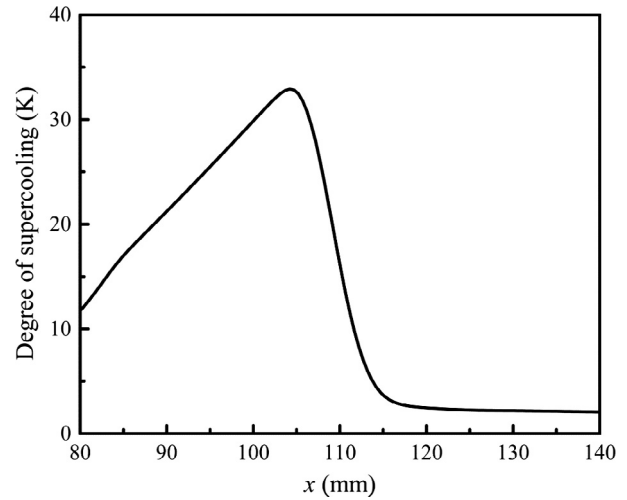**Fig. 5.** Numerical and experimental results of droplet fraction at the central line of the Laval nozzle.
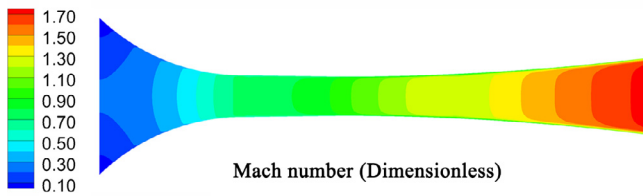

Fig. 6. Mach number contours in the Laval nozzle.

center line is described in Fig. 7. It can be observed that the vapor accelerates to a supersonic speed and correspondingly results in the increase of the Mach number. However, the Mach number starts to decrease, when the spontaneous condensation of water vapor occurs. This can be explained that the change of the latent heat between the phase transition process from the vapor to liquid will heat the water vapor. After that, the steam expands again, and the Mach number increases in the diverging part of the Laval nozzle.

Figs. 8 and 9 show the degree of supercooling and nucleation rate during the water vapor condensation process. We can see that the supercooling degree increases constantly along with the vapor expansion, and it rapidly rises to the peak value of about 33 K in
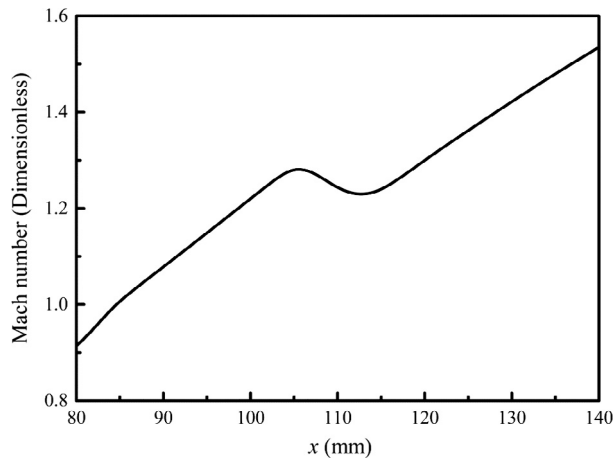

Fig. 7. Mach number at the central line of the Laval nozzle.

Fig. 8. Degree of supercooling at the central line of the Laval nozzle.
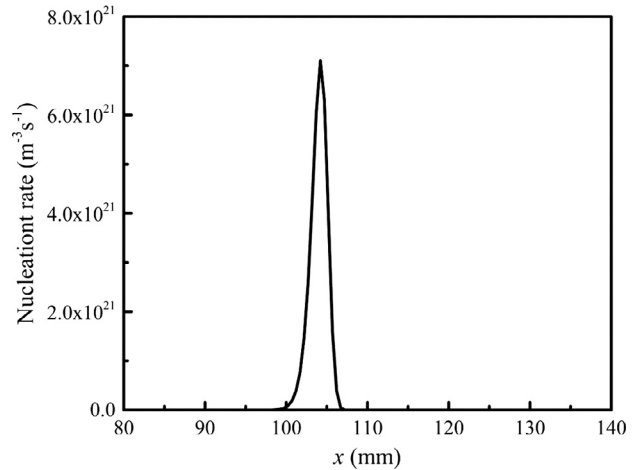

Fig. 9. Nucleation rate at the central line of the Laval nozzle.

this case. In this condition, the steam is in an extremely non-equilibrium thermodynamic state, leading to the occurrence of the spontaneous condensation in a very short moment, which can be observed in Fig. 9. The degree of supercooling then suddenly decreases from 33 K to 2 K, which means that the condensation process has finished.

Fig. 9 obviously reflects the nucleation process of water vapor in supersonic flows. The nucleation process starts to occur approximately at $x = 100$ mm, and sharply rises from 0 to 7.2×10^{21} m^{-3} - s^{-1} in a very short time. It means that a massive number of condensation nuclei appear in the steam. In a short while, the nucleation rate drastically declines from peak to zero because of the decrease of the supercooling degree. It indicates that the water vapor will not spontaneously condense at once when the steam reaches the saturation state. On the contrary, the nucleation phenomenon occurs somewhere downstream the nozzle throat, and shows a rapid variation both in space and in time.

The distribution of the droplet numbers at the center line of the Laval nozzle is shown in Fig. 10. The vapor molecules constantly collide with each other and coalesce, and continuingly produce the critical nucleus, when the spontaneous condensation starts to occur. Under this thermodynamic condition, a large number of droplets will appear when the condensation nucleus reaches a certain quantity and goes into the droplet growth process. The droplet
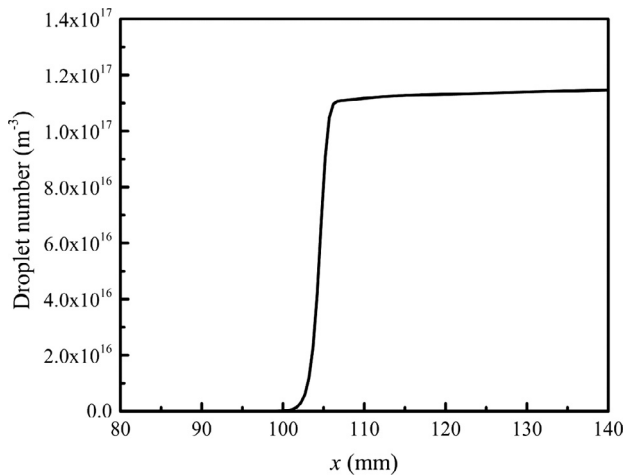
Fig. 10. Droplet numbers at the central line of the Laval nozzle.

Fig. 12. Droplet fraction of at the central line of the Laval nozzle.

numbers also rapidly rise from 0 to 1.12×10^{17} in a very short distance due to the sharp process of the vapor nucleation. Then, the steam is almost back to the equilibrium state because of the decrease of the supercooling degree. At that moment, no new condensation nucleui appear and the droplet number remains effectively unchanged.

Figs. 11 and 12, respectively, show the radius and mass fraction of the droplet at the center line of the Laval nozzle. The large numbers of vapor molecules are able to aggregate on the droplet surface, when the nucleation rate and droplet numbers reach the peak. The radius and mass fraction of the droplet also begin to rapidly increase as a result of the large number of the condensing nuclei and droplet numbers. It also can be seen that the increase of the droplet mass fraction lags behind the change of the droplet radius by comparing Figs. 11 and 12. It means that the droplet radius changes in the first place and then the droplet fraction grows dramatically. Combining Figs. 8 and 9, we also find that the vapor molecules can still continue to aggregate on the droplet surface due to the supercooling degree at about 2 K, when the droplet number remains unchanged. Therefore, the radius and mass fraction of the droplet increase continuously till the nozzle outlet as a result of the state of supersaturation.
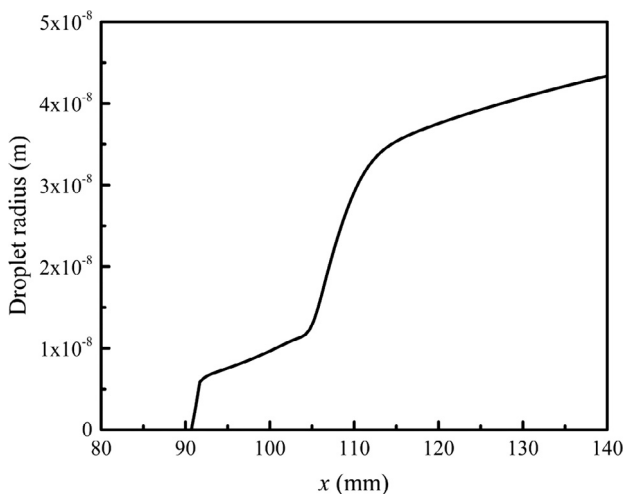
4. Conclusions

The condensation process of water vapor in the Laval nozzle is simulated numerically with the nucleation and droplet growth theories. The results show that the latent heat is released to heat into the vapor phase during the spontaneous condensation, leading to the jump of the condensing parameters. The degree of supercooling can reach a maximum value of about 33 K and correspondingly the spontaneous condensation occurs in a very short time. The droplet numbers also rapidly rise from 0 to 1.12×10^{17} in a very short moment. Then, the radius and mass fraction of the droplet also begin to increase continuously till the nozzle outlet as a result of the supercooling degree at about 2 K.

Acknowledgements

References

[1] S.J. Keisari, M. Shams, Shape optimization of nucleating wet-steam flow nozzle, Appl. Therm. Eng. 103 (2016) 812–820.
[2] Y. Patel, G. Patel, T. Turunen-Saaresti, Influence of turbulence modelling on non-equilibrium condensing flows in nozzle and turbine cascade, Int. J. Heat Mass Transfer 88 (2015) 165–180.
[3] N. Sharifi, M. Boroomand, M. Sharifi, Numerical assessment of steam nucleation on thermodynamic performance of steam ejectors, Appl. Therm. Eng. 52 (2013) 449–459.
[4] S.M.A. Noori Rahim Abadi, R. Kouhikamali, K. Atashkari, Non-equilibrium condensation of wet steam flow within high-pressure thermo-compressor, Appl. Therm. Eng. 81 (2015) 74–82.
[5] C. Wen, A. Li, J.H. Walther, Y. Yang, Effect of swirling device on flow behavior in a supersonic separator for natural gas dehydration, Sep. Purif. Technol. 168 (2016) 68–73.
[6] C. Wen, Y. Yang, J.H. Walther, K.M. Pang, Y. Feng, Effect of delta wing on the particle flow in a novel gas supersonic separator, Powder Technol. 304 (2016) 261–267.
[7] Y. Yang, A. Li, C. Wen, Optimization of static vanes in a supersonic separator for gas purification, Fuel Process Technol. 156 (2017) 265–270.
[8] Y. Yang, C. Wen, CFD modeling of particle behavior in supersonic flows with strong swirls for gas separation, Sep. Purif. Technol. 174 (2017) 22–28.
[9] Y. Yang, C. Wen, S. Wang, Y. Feng, P. Witt, The swirling flow structure in supersonic separators for natural gas dehydration, RSC Adv. 4 (2014) 52967–52972.
[10] S. Dykas, M. Majkut, M. Strozik, K. Smołka, Experimental study of condensing steam flow in nozzles and linear blade cascade, Int. J. Heat Mass Transfer 80 (2015) 50–57.

Fig. 11. Droplet radius at the central line of the Laval nozzle.

[11] H. Ding, C. Wang, Y. Zhao, An analytical method for Wilson point in nozzle flow with homogeneous nucleating, Int. J. Heat Mass Transfer 73 (2014) 586–594.

[12] C. Moses, G. Stein, On the growth of steam droplets formed in a Laval nozzle using both static pressure and light scattering measurements, J. Fluids Eng. 100 (1978) 311–322.

[13] P.G. Hill, Condensation of water vapour during supersonic expansion in nozzles, J. Fluid Mech. 25 (1966) 593–620.

[14] S.M.A. Noori Rahim Abadi, R. Kouhikamali, K. Atashkari, Two-fluid model for simulation of supersonic flow of wet steam within high-pressure nozzles, Int. J. Therm. Sci. 96 (2015) 173–182.

[15] A. White, J. Young, Time-marching method for the prediction of two-dimensional, unsteadyflows of condensing steam, J. Propul. Power 9 (1993) 579–587.

[16] A. Gerber, Two-phase Eulerian/Lagrangian model for nucleating steam flow, J. Fluids Eng. 124 (2002) 465–475.

[17] M.R. Mahpeykar, A. Taymourtash, The effects of friction factor and inlet stagnation conditions on the self condensation of steam in a supersonic nozzle, Sci. Iranica 11 (2004) 269–284.

[18] W. Jiang, Z. Liu, H. Liu, H. Pang, L. Bao, Influences of friction drag on spontaneous condensation in water vapor supersonic flows, Sci. China Ser. E: Technol. Sci. 52 (2009) 2653–2659.

[19] D. Simpson, A. White, Viscous and unsteady flow calculations of condensing steam in nozzles, Int. J. Heat Fluid Flow 26 (2005) 71–79.

[20] Y. Yang, S. Shen, Numerical simulation on non-equilibrium spontaneous condensation in supersonic steam flow, Int. Commun. Heat Mass Transfer 36 (2009) 902–907.

[21] B. Nikkhahi, M. Shams, M. Ziabasharhagh, A numerical study of two-phase transonic steam flow through convergence-divergence nozzles with different rates of expansion, Kor. J. Chem. Eng. 27 (2010) 1646–1653.

[22] S. Dykas, W. Wróblewski, Numerical modelling of steam condensing flow in low and high-pressure nozzles, Int. J. Heat Mass Transfer 55 (2012) 6191–6199.

[23] A.H. Yousif, A.M. Al-Dabagh, R.C. Al-Zuhairy, Non-equilibrium spontaneous condensation in transonic steam flow, Int. J. Therm. Sci. 68 (2013) 32–41.

[24] S.L. Girshick, C.P. Chiu, Kinetic nucleation theory: a new expression for the rate of homogeneous nucleation from an ideal supersaturated vapor, J. Chem. Phys. 93 (1990) 1273–1277.

[25] G. Gyarmathy, The spherical droplet in gaseous carrier streams: review and synthesis, Multiphase Sci. Technol. 1 (1982) 99–279.

[26] C. Wen, X. Cao, Y. Yang, Y. Feng, Prediction of mass flow rate in supersonic natural gas processing, Oil Gas Sci. Technol. 70 (2015) 1101–1109.

[27] C. Wen, X. Cao, Y. Yang, W. Li, An unconventional supersonic liquefied technology for natural gas, Energy Educ. Sci. Technol. Part A Energy Sci. Res. 30 (2012) 651–660.

[28] Y. Yang, C. Wen, S. Wang, Y. Feng, Numerical simulation of real gas flows in natural gas supersonic separation processing, J. Nat. Gas Sci. Eng. 21 (2014) 829–836.

[29] Y. Yang, C. Wen, S. Wang, Y. Feng, Effect of inlet and outlet flow conditions on natural gas parameters in supersonic separation process, PLoS ONE 9 (2014) e110313.

[30] F.R. Menter, Two-equation eddy-viscosity turbulence models for engineering applications, AIAA J. 32 (1994) 1598–1605.

[31] S.V. Patankar, D.B. Spalding, A calculation procedure for heat, mass and momentum transfer in three-dimensional parabolic flows, Int. J. Heat Mass Transfer 15 (1972) 1787–1806.